High Speed Large Format Photon Counting Microchannel Plate Imaging Sensors

Oswald H. W. Siegmund, Camden Ertley, John V. Vallerga,
Space Sciences Laboratory, U.C. Berkeley
Chris A. Craven, Mark A. Popecki, Aileen O'Mahony, Michael J. Minot
Incom Inc., Charlton, MA

ABSTRACT

The development of a new class of microchannel plate technology, using atomic layer deposition (ALD) techniques applied to a borosilicate microcapillary array, is enabling the implementation of larger, more stable detectors for Astronomy and remote sensing. Detectors have been developed to cover a wide range of optical/UV sensing applications. Formats of 25mm circular, and 50mm (Planacon) and 200mm square have been constructed, with potential uses from night time remote reconnaissance and biological single-molecule fluorescence lifetime imaging microscopy, to large area focal plane imagers for astrophysics, neutron detection and ring imaging Cherenkov detection. The large focal plane areas were previously unattainable, but the new developments in construction of ALD microchannel plates allow implementation of formats of 20cm or more. Continuing developments in ALD microchannel plates offer improved overall lifetime and gain stability up to 7 C cm^{-2} of charge extraction. Furthermore, they show reduced levels of background, as low as 0.028 events cm^{-2} sec^{-1} and have low gamma ray detection efficiency for use in high radiation environments. Conversely, UV photon and electron detection efficiencies are high. The gain is also high, with narrow saturated pulse height distributions, and curved surface MCP formats are also under development.

Keywords: Microchannel plate, photon counting, imaging, timing

1. INTRODUCTION

A depiction of a microchannel plate (MCP) detector scheme is shown in Fig. 1. In this "sealed tube" device the radiation passes through the input window and is converted to photoelectrons by a photocathode. The emitted photoelectrons are amplified by a pair, or triplet, of MCPs which are then detected by a readout anode that is a pattern of conductive strips, in both X and Y directions. We have used these devices as photon counting, imaging, event time tagging detector schemes for a number of astronomical [1-6], remote sensing [7], time resolved biological imaging [8, 9], photoelectron emission spectroscopy [10] and night time sensing [11] applications. The development of large area, high performance, photon counting, imaging, timing detectors also has significance for "open faced" configurations for UV and particle detection in space astrophysics, mass spectroscopy and many time-of–flight applications. Furthermore, sealed tube configurations for optical/UV sensing also have applications in detection of Cherenkov light (RICH), scintillation detection, and neutron imaging applications

We have been investigating MCPs [12] made by atomic layer depositions (ALD) on borosilicate micro-capillary arrays as a means of advancing detector performance beyond that available with conventional MCPs. ALD MCPs have many performance characteristics typical of conventional microchannel plates [12], however in some aspects they show distinct improvements. ALD borosilicate MCPs have been tested, mainly in a 33mm format but we have also assessed ALD MCPs up to 20 cm format, as conventional MCPs of this size are not available. ALD MCPs have shown low intrinsic background [13,14] (<0.07 events cm^{-2} s^{-1}), low outgassing during preconditioning vacuum bake [13], and virtually no gain degradation over at least 7 C cm^{-2} of charge extraction [13] after a vacuum bake. We have now made measurements with a new borosilicate substrate glass that offers improvements beyond what we have achieved to date and discuss lifetest results for sealed tube detectors made with ALD MCPs. One sealed device is a PHOTONIS Planacon 32 x 32 anode device, and the other is a sealed tube 25mm detector with a cross delay line readout and a GaN opaque photocathode deposited onto the front MCP. Results for the quantum efficiency, stability, radiation sensitivity and gain / pulse amplitude distributions for the new ALD borosilicate glass and MCPs are presented below.

2. ATOMIC LAYER DEPOSITED BOROSILICATE SUBSTRATE MICROCHANNEL PLATES

Atomic layer deposited microchannel plates are based on a scheme where a borosilicate micro-capillary array substrate can be configured to function as a microchannel plate by deposition of resistive and secondary emissive layers using atomic layer deposition. The process establishes an extremely robust substrate at reduced cost, and allows very

large microchannel plates to be produced with pore sizes as small as 10 microns. The process begins with glass tubes that are stacked and fused in a similar way to standard MCPs, however no core glass etching is required. The major visible structures (Fig. 2) of these MCPs are the hexagonal patterns which represent the initial fused stacking blocks for the glass tubes. Many of these are used to make a full size MCP, and when fused together some of the glass tubes (pores) at the hexagonal interfaces deform slightly. The robustness and flatness of the MCPs using borosilicate microcapillary arrays is excellent, and is due in part to the resilience and stability of the substrate material and its high temperature properties (~700°C softening point). Deposition of resistive and secondary emissive layers onto the substrate with the ALD process, followed by evaporation of NiCr electrodes complete the MCP fabrication process. The resistance of MCPs fabricated to date has ranged from <5 MΩ to >1 GΩ, and either Al_2O_3 or MgO have been used to achieve the high secondary emission coefficient electron multiplication layers.

Initial tests of the ALD MCPs were performed on 33 mm MCPs [13,15] that showed many of the performance characteristics are typical of conventional microchannel plates [12]. However, the background rates are lower than conventional MCPs because the borosilicate glass contains less radioactive material than standard MCP glass formulations. We have also found that in pre-conditioning steps on borosilicate ALD microchannel plates the MCP gain can rise by an order of magnitude after a vacuum bake [13] and then remain stable [13] during burn-in up to 7 C cm^{-2}. Most recently a 2nd generation of borosilicate glass substrate has been implemented with higher resiliency, larger pore open area ratios and better chemical compatibility with coatings and photocathode depositions. We will discuss the results of our evaluations of the new glass and of further measurements with the original composition.

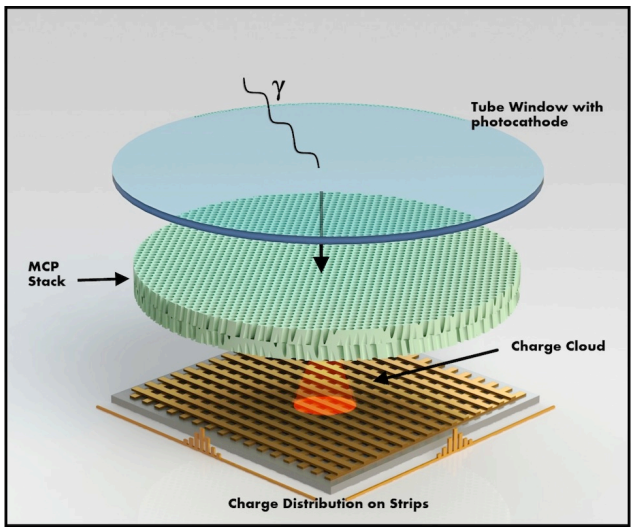

Fig. 1. An MCP imaging sensor scheme. A photocathode is deposited on a window facing a pair of MCPs. Emitted photoelectrons are detected by the MCPs and collected by several strips in each axis of the anode to encode positions.

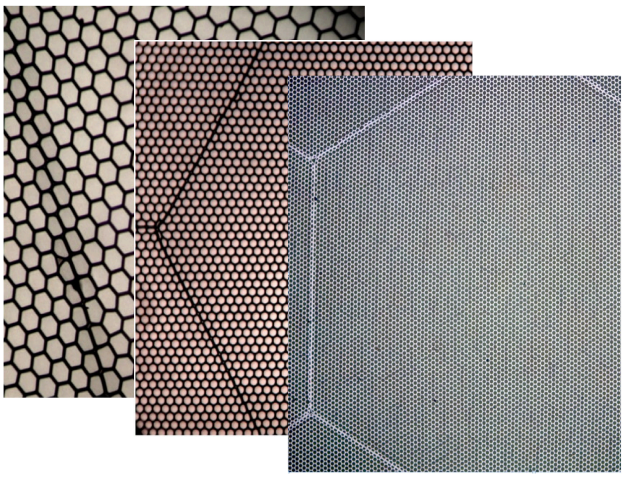

Fig. 2. Configuration of microchannel plate borosilicate substrates. Left MCP 40µm pore 80% open area, center 20 µm pores with a 65% open area, right 10 µm pores 60% open area, 60:1 pore L/d, and 8° pore bias angle.

2.1 Large Area ALD Microchannel Plate Detectors

To accomplish detailed assessment of 20 cm MCPs we have utilized an open face detector with a 20 cm cross delay line anode for event position encoding (Fig. 3). Encoding the difference in signal arrival times at each end of two orthogonal delay lines allows photon positions in each axis to be determined, and the 20 cm area cross delay line readout has an end to end signal propagation of ~130 ns. The detector scheme provides event by event accumulated images and gain map images for the MCPs that can be used to characterize the efficiency, overall uniformity, background rate and spatial resolution of the 20 cm ALD MCPs when used in a pair (Fig. 1) or triple stack configuration. Other configurations are being developed, specifically curved surface MCPs that can match instrument focal planes that are cylindrical or spherical. Initial steps in this development show that even large format substrates can be made highly curved (Fig. 4) with acceptable fidelity. Efforts are currently underway to provide fully operational MCPs in these curved configurations.

2.2 Imaging Tests with Large Area Atomic Layer Deposited Microchannel Plates

Tests with 33mm round format ALD MCPs on borosilicate substrates have established that the gain, pulse amplitude distribution, and MCP resistance are similar to conventional MCPs [12]. Similar tests on 20 cm square MCPs have been done, using the standard format of 20 µm pores, 60:1 L/d, and with an 8° pore bias angle. With a 200 V bias

applied across a 0.75mm inter-MCP gap and a,~1000 V applied to each MCP, we routinely obtain ~ 5 x 10^6 gain and a peaked pulse amplitude distribution [13]. The gains with the 20 cm ALD MCP pairs can reach 10^7 or greater. With the large area format there are often problems with the spatial uniformity of the operating characteristics [13] due to intrinsic variations in the multiplication process or simply the physical flatness of the MCPs. Both of these issues have been addressed and good performance data can be achieved. A gain map image containing > 10^8 events (Fig. 5) shows the gain uniformity over the entire area is better than 15%. Image quality tests using the 20 cm detector with 3 MCPs in a stack with the a cross delay line readout (Fig. 7) at 8k x 8k pixel binning show an overall pattern of striations. Mottling and striations of the gain map image in Fig. 7 are due to the small gain variations for individual MCP hexagonal multifibers that can be seen on the magnified inset, in common with conventional MCPs. These images can be accumulated at event rates of up to ~1 MHz, and provide useful information on individual MCP ALD processing.

The background rate for borosilicate ALD MCPs is low (<0.07 events cm^{-2} s^{-1}) compared to conventional MCPs [13] and is due to low intrinsic radioactivity in the glass. In large size formats particulates and surface damage can cause local field emission (hot spots). However, we have been able to measure the background rate for 20 cm MCPs that do have some debris, but show little or no signs of hot spot activity. In such MCPs we can see that the background rate (Fig. 6) can be very low, about 0.028 events cm^{-2} sec^{-1} for the general 400 cm^2 area, excluding 2 or 3 "warm spots". This level is comparable with the expected rate due to cosmic ray muon events and is as low as can be envisioned without precautions to shield the detector from external radiation.

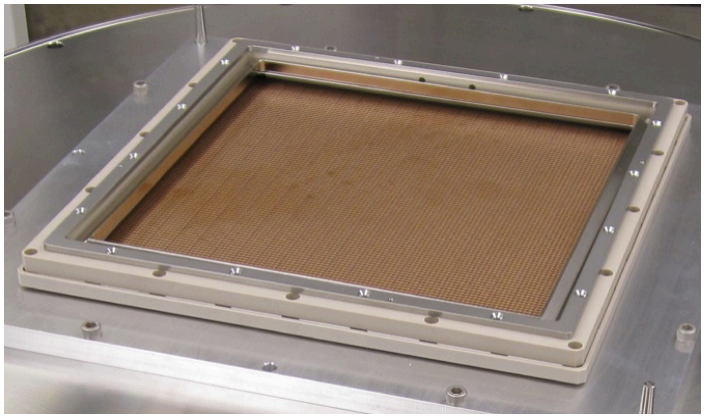

Fig. 3: 20 cm cross delay line readout detector (without MCPs) used for tests of 20 cm ALD MCPs in pairs or triplets.

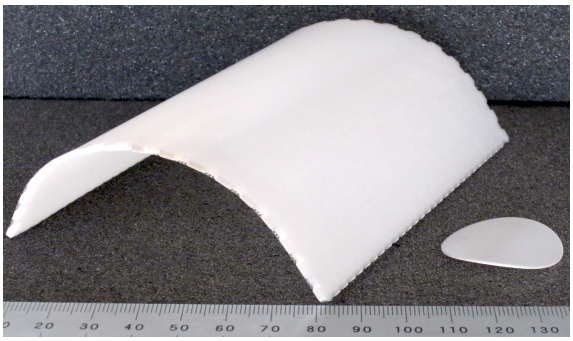

Fig. 4: Curved surface Borosilicate MCP substrates 12 x12 cm, 4.5cm radius & 33mm, 7.5cm radius.

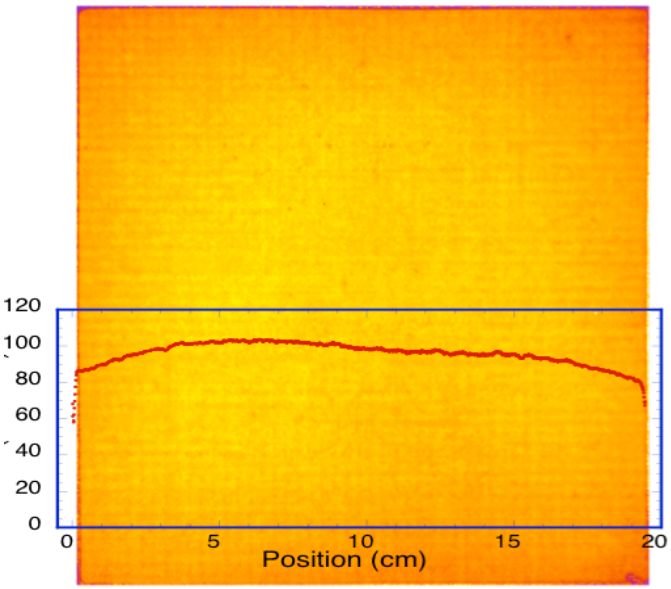

Fig. 5. Average gain image "map" (<15% variation). 20cm MCP pair, 20µm pore, 60:1 L/d ALD MCPs ~7x10^6 gain, 0.7 mm inter-MCP gap/200v.

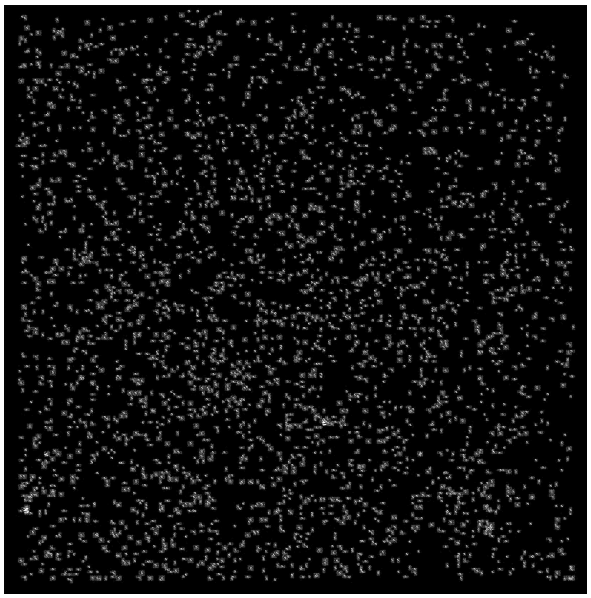

Fig. 6. 300 sec background image. 20µm pore, 60:1 L/d ALD-MCP pair. General background is low (0.028 sec^{-1} cm^{-2}) due to the absence of lead, and reduced amounts of ^{40}K in the borosilicate glass.

Spatial resolution of the 20cm detector was assessed with the current generation of time to digital electronics using 13 bit electronic position coordinate binning. With this readout, resolution of about 60 µm FWHM has been achieved (Fig. 8) provided the MCP gain is sufficiently high (1.5 x 10^7). Better spatial resolution (25µm) [14] has been achieved with cross strip readouts, but only up to 100 mm format to date. The cross delay line readout is simpler to make and implement, with a less complex set of electronics, so should provide a viable scheme for many applications. In addition event time tagging to the 100ps level is accommodated.

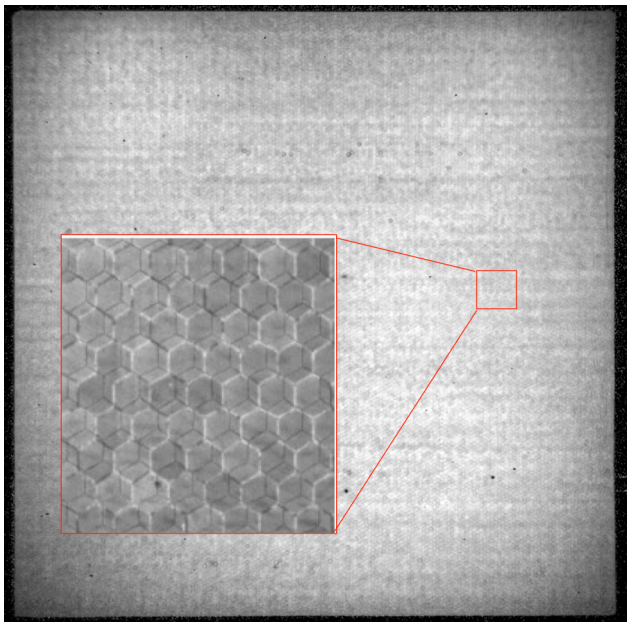

Fig. 7. UV illuminated (184 nm) gain map image for a 20 cm MCP 3 stack. Gain ~1.5 x 10^7, 20 µm pores, 60:1 L/d. Zoomed inset shows the hexagonal MCP multifiber gain.

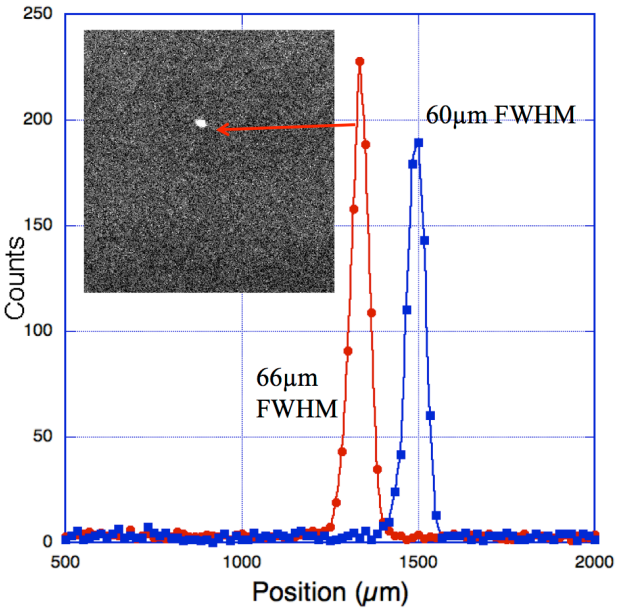

Fig. 8 Spatial resolution demonstration for a 20cm ALD MCP triplet with 20µm pores, gain ~1.5 x 10^7, 8° bias, 60:1 L/d. 20cm cross delay line readout showing ~60µm FWHM resolution.

2.3 Performance Testing With 2nd Generation Borosilicate ALD Microchannel Plates

At the inception of the ALD MCP technique, 33mm round format ALD MCPs with the original borosilicate substrates were extensively used to establish that the gain, pulse amplitude distribution, and MCP resistance are similar to conventional MCPs [12]. The background rates (~0.07 events cm^{-2} sec^{-1}, [13]) were found to be substantially lower than conventional MCPs as the borosilicate glass has less potassium than conventional MCP glass compositions (lower ^{40}K beta rate). Preconditioning steps (bake, burn-in) on 33mm borosilicate ALD microchannel plates [12] showed that vacuum baking or burn-in causes an asymptotic gain increase for MgO coated ALD MCPs, which can then remain stable for up to 7 C cm^{-2} at gains of ~10^6 [14].

A second generation of borosilicate substrate material has come into use and we have tested this in 33mm format to affirm its compatibility with ALD processes. The chemical composition of the new borosilicate glass is potentially better for several performance parameters. The open area ratio of the glass tubes is normally higher and there is less alkali metals in the glass. Initial gain tests show a consistently high gain (Fig. 9) in the standard format of 20 µm pore, 60:1 L/D, 8° bias angle and 74% open area. One consequence of high gain is a better pulse height saturation leading to narrower pulse amplitude distribution widths at the higher gains used for single event counting detector systems with MCP stacks. This can be seen in Fig. 10 for ALD MCPs as compared with a similar MCP stack of conventional glass MCPs. Even with large area ALD MCPs where gain variations across the active area can degrade the pulse amplitude distribution, the overall performance is reasonable with the 1st generation borosilicate glass (Fig. 11) and the background rates are exceptional (Fig. 6) (peak in the background distribution (Fig. 11) at ~6 x 10^6 gain is due to "warm spots" on the MCP surface).

The quantum detection efficiency of "bare" MCPs is a good indicator of MCP performance and the final detection efficiency when coated with a photocathode material. Measurements of the ALD MCP quantum detection efficiency on samples of two batches of MCPs (Fig. 12) indicate a consistently higher efficiency than historical (HST-COS [5]) and recent conventional MCP (std 12µm MCP) efficiencies. This may be partly as a result of the increased open area ratio for the ALD substrates, the effect of the secondary emission coefficients, or both.

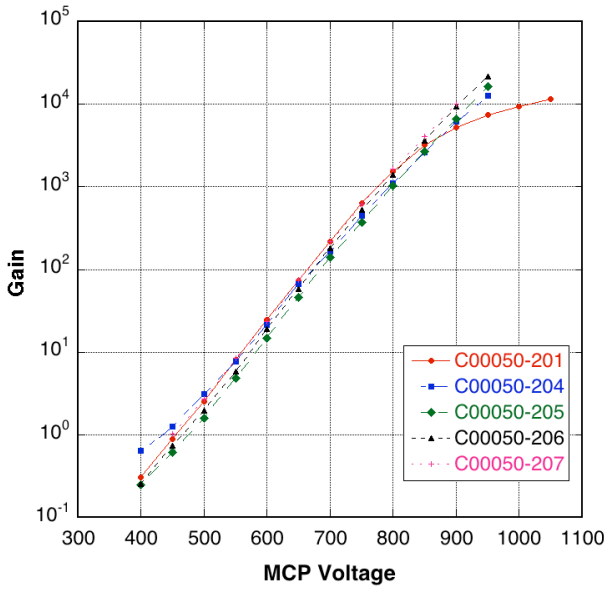

Fig. 9. Gain characteristics of 33 mm diameter Al_2O_3 coated borosilicate MCPs, 20 µm pore, 74% open area, 60:1 L/D, 8° bias angle.

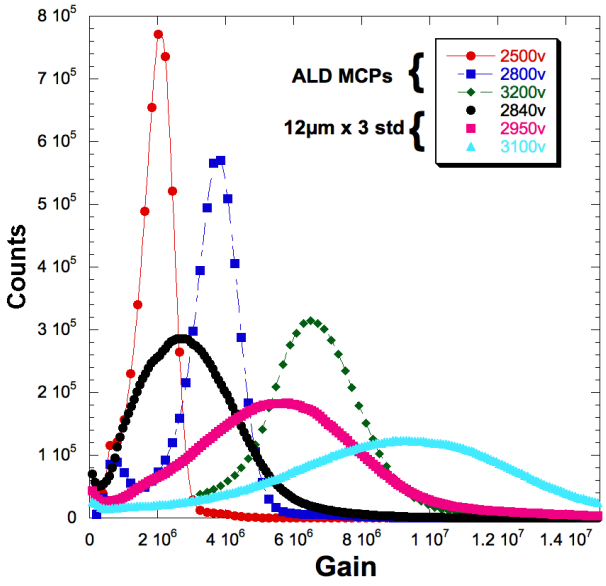

Fig. 10: Pulse height spectra for UV with ALD MCPs are narrower than standard MCPs. ALD MCP triplet (33mm, 20µm pore, 60:1 L/d, 8° bias) with MgO emissive layer.

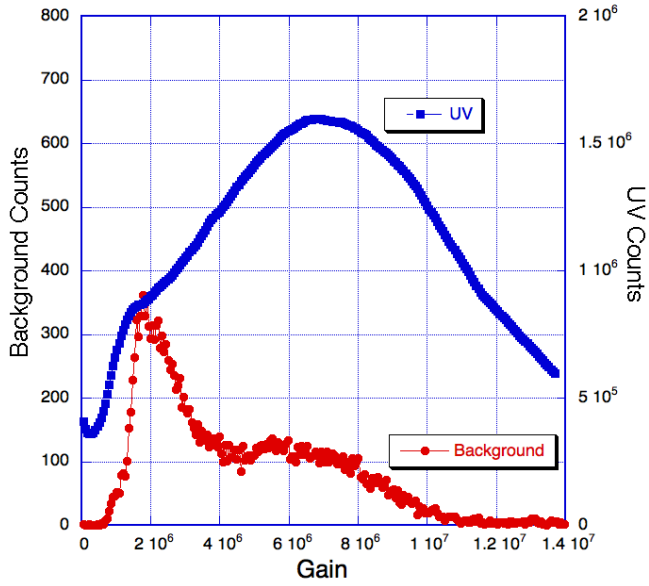

Fig. 11. Gain pulse height spectra for UV & background events, 200mm mm diameter Al_2O_3 coated borosilicate MCP pair, 20 µm pores, 60:1 L/D, 8° bias.

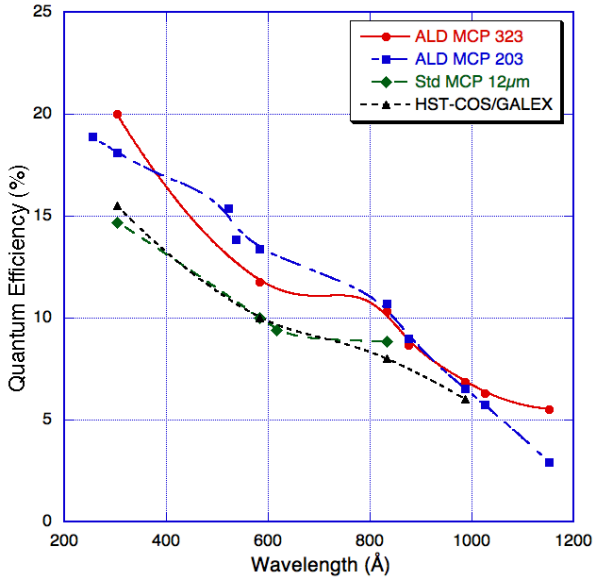

Fig. 12: ALD MCP quantum efficiency for 74% open area ALD MCPs with Al_2O_3 emissive layer, 20µm pore, 60:1 l/d, 8° bias angle, compared with standard MCPs.

Another important factor in implementation of MCP detectors, specifically in space instrumentation and high energy physics applications, is their sensitivity to penetrating radiation. In this respect we have made a preliminary assessment to determine the sensitivity of ALD borosilicate MCPs to ~1 MeV gamma rays and electrons. A ^{90}Sr ß decay source was used in close proximity (<5mm) to a pair of ALD MCPs to measure the efficiency and pulse height spectrum for electron energies in the range ~50keV to ~1MeV. The pulse amplitude distribution shows a peak close to the UV event modal gain peak, but has a higher gain tail that is indicative of the increased number of electrons emitted as a result of the high energy ß event interactions in the bulk of the MCP glass. The derived efficiency of ~47% is in close correlation with the efficiency we obtain for the same test done with conventional MCPs. This is generally consistent with the expectations for detection of 90Sr ß's from the cross sections of the MCP materials. The data available for γ ray detection by MCPs suggests that the efficiency is ~2% [16] over the 500 KeV- 5 MeV region. Using a ^{60}Co

γ ray source we have measured the rate and pulse height spectrum for ~1MeV γ ray detection by 2nd generation borosilicate ALD MCPs.

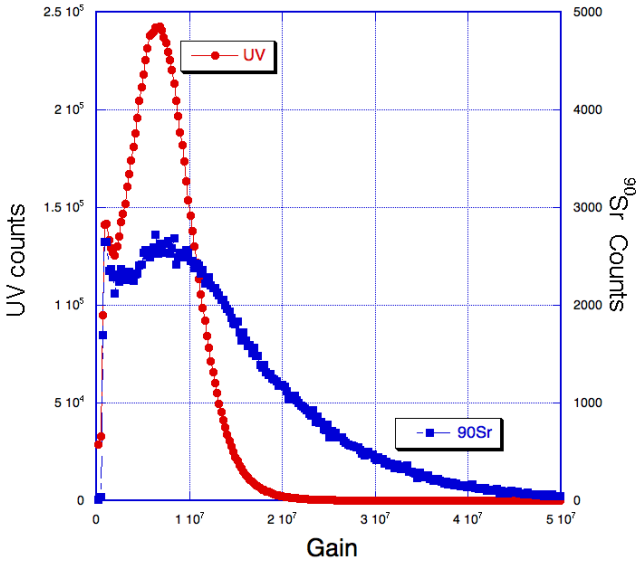

Fig. 13. ALD MCP pair (33mm, 20µm pore, 60:1 L/d, 8° bias) with MgO emissive layer. Pulse height spectra for UV and ^{90}Sr ß (~47% detection efficiency).

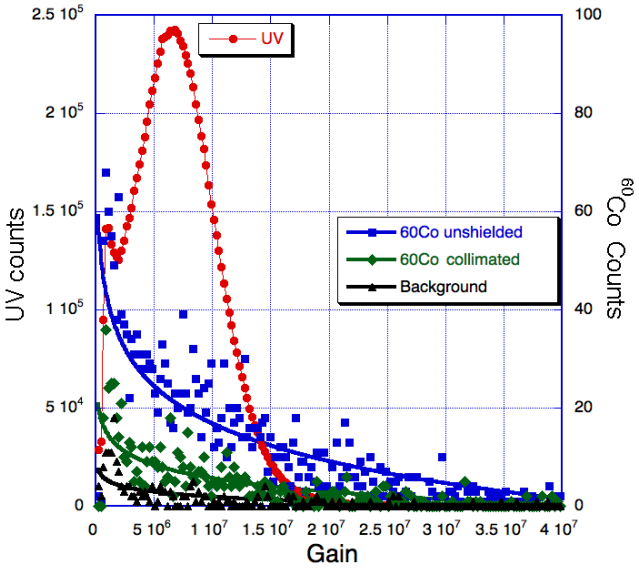

Fig. 14: ALD MCP pair (33mm, 20µm pore, 60:1 L/d, 8° bias) with MgO layer. Pulse height spectra for UV and ^{60}Co γ (~0.25% efficiency for collimated beam).

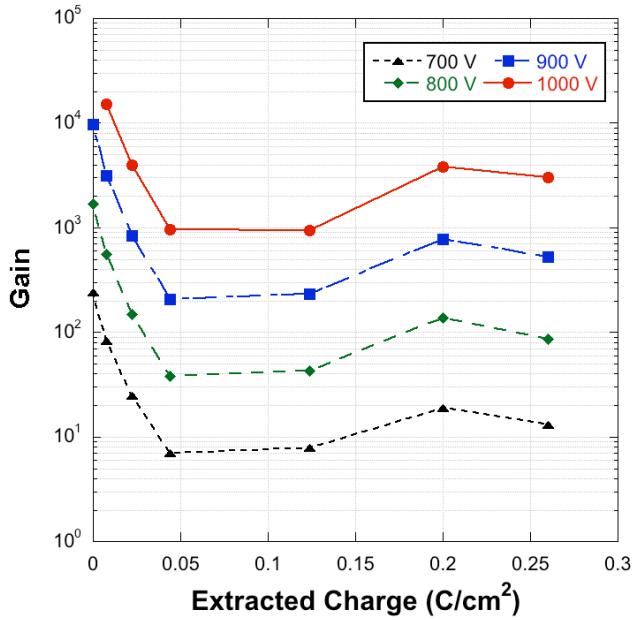

Fig. 15. Burn-in (200 eV e$^-$) of ALD MCPs (33mm, 20µm pore, 60:1 L/d, 8° bias) with Al_2O_3 emissive layer (No vacuum pre-bake).

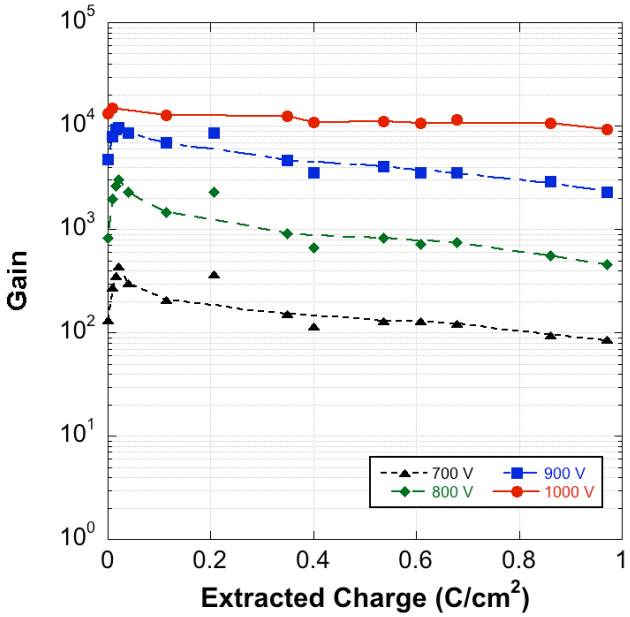

Fig. 16: Burn-in (200 eV e$^-$) of ALD MCPs (33mm, 20µm pore, 60:1 L/d, 8° bias) with MgO emissive layer (No vacuum pre-bake).

The initial pulse height and detection rate data was taken with an unshielded ^{60}Co source in proximity to the MCP detector and yielded a negative exponential pulse height spectrum as compared with the peaked pulse height spectrum for UV radiation (Fig. 14). The overall rate indicated a ~1% detection efficiency for ~1 MeV gamma rays above the ambient background level. This is somewhat less than the historical values for standard MCPs (2%), which also compare with our previous measurements for conventional MCPs (3%)[17]. However, there is considerable interaction with surrounding vacuum chamber and detector structures that can expose the MCPs to detection of secondary and scattered radiation. We also implemented source collimation so that the γ rays would impinge only on the MCPs and structures in the direct path. In this case we see a distinct drop in the detection efficiency, giving an upper limit of

~0.25%, which is still potentially affected by remaining materials immediately around and behind the MCPs. Further studies are in progress, but for ALD borosilicate MCPs this reduction has potential benefits in reducing gamma ray background in high radiation environments.

Initial investigation of the gain stability of the second generation of borosilicate substrate material was done for both MgO and Al_2O_3 emissive layers on ALD MCPs. Generally Al_2O_3 coated MCPs show a decline in gain with charge extraction [13], and we do see an initial decrease (Fig. 15) with the newer ALD MCPs. However, the gain then substantially increases again at ~0.2 C cm^{-2}. This test is continuing to establish the gain trend out to 1 C cm^{-2} and beyond. The gain trend for MgO ALD MCPs has been previously shown to increase considerably as charge is extracted [13] or if the MCPs are vacuum baked at high temperature. The current data with second generation of borosilicate substrate material indicates (Fig 16) that at nominal gain of 10^4 the gain remains stable up to 1 C cm^{-2} without any substantive changes. At lower gains there is a slight drop-off however. The effects of a high vacuum bake are yet to be determined with the second generation of borosilicate substrates. The possibility of gain stability, with or without a vacuum bakeout, is extremely attractive for both sealed tube and open face devices in many applications.

3. SEALED TUBES WITH ALD MCPS

The properties of ALD MCPs make them potentially attractive for sealed tube devices with novel photocathode materials. To date, two sealed tubes have been made, a 33mm round tube with an opaque GaN photocathode (Fig. 17) and a 50mm Planacon with ALD MCPs (Fig. 21). In addition a collaboration (Large Area Picosecond Photon Detector) consisting of the U. Chicago, Argonne National Laboratory, U.C. Berkeley, U. Hawaii, Incom. Inc., and several other institutions have been developing novel ALD borosilicate MCP technologies to realize a 20 cm square format sealed tube detector [12].

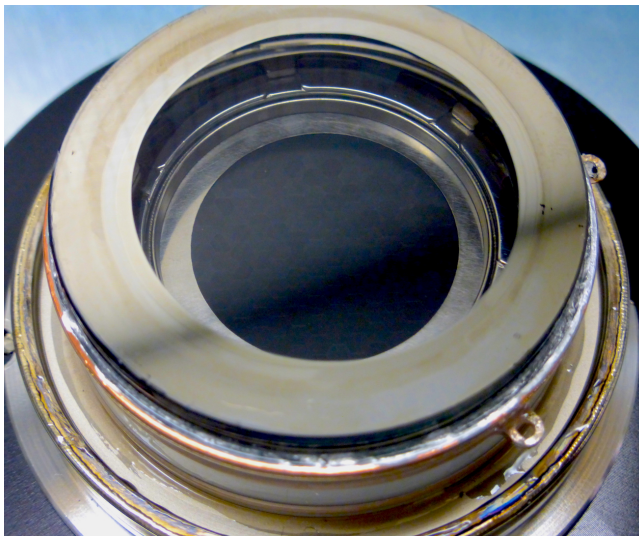

Fig. 17. 25 mm sealed tube with a GaN photocathode directly deposited onto a pair of borosilicate substrate ALD coated MCPs (20µm pore, 60:1 l/d). XDL readout.

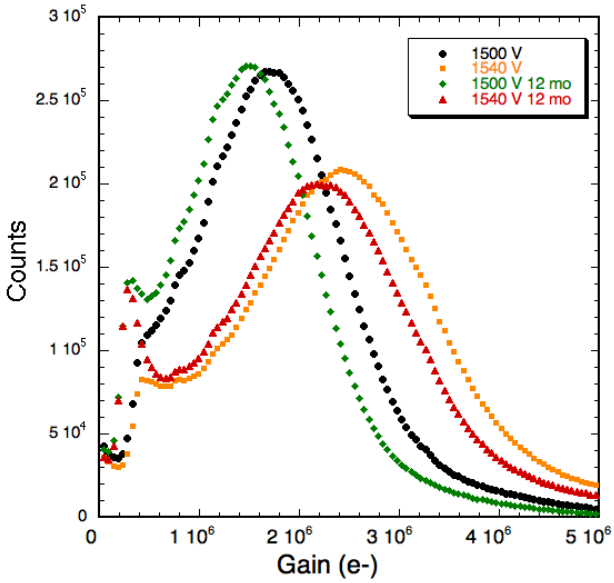

Fig. 18: ALD MCP sealed tube pulse height distribution with 184nm UV, GaN coated ALD MCPs 20µm pore, 60:1 l/d, 8° bias. Little change over 12 months.

3.1 GaN Sealed Tube Construction and Photocathode Development

A cross delay line readout (25mm) sealed tube (Fig. 17) [18] was made to test a GaN photocathode deposited onto ALD MCPs. This uses a hot indium seal to a magnesium fluoride entrance window and a brazed ceramic/metal vacuum housing. The ALD MCP capability of sustaining much higher temperatures than standard MCPs accommodated the GaN (Mg) deposition (SVT Inc.) [19] by Molecular Beam Epitaxy onto the top surface of the upper MCP. The pair of 33mm 60:1 l/d, 20 µm pore ALD borosilicate MCPs achieved gains of $>10^6$ and the MCP gain rose about one order of magnitude during vacuum bake. During a short "burn-in" (<0.05 C cm^{-2}) very little gas was observed to be released and there was no gain decrease. The GaN photocathode was activated by deposition of Cs to lower the GaN work function and the final step in tube processing was the MgF_2 window seal (hot indium).

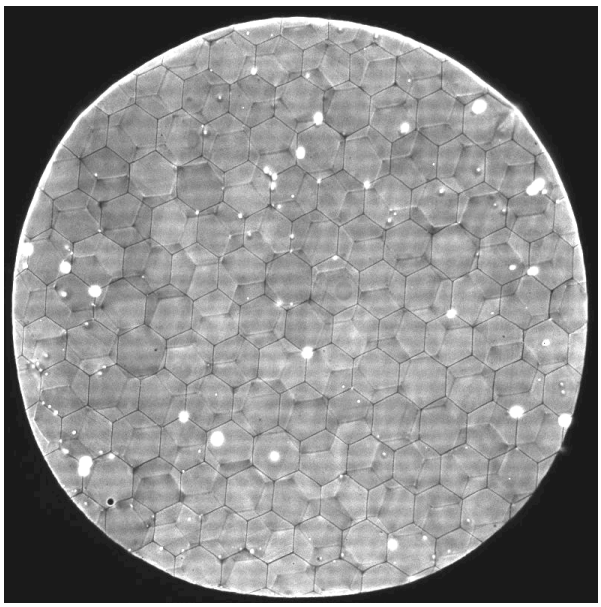

Fig. 19: 184nm UV illuminated image for 25mm opaque GaN ALD MCP sealed tube. MCP multifibers, and hotspots due to particulates are visible in the image.

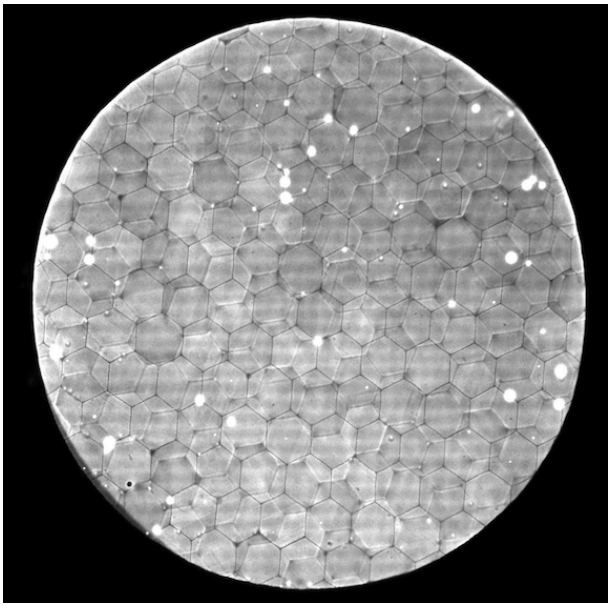

Fig. 20: 184nm UV illuminated image for 25mm opaque GaN ALD MCP sealed tube after 12 months. Few changes and overall behavior is similar.

The completed sealed tube has a good single photon pulse amplitude distribution [20] and gains up to ~5 x 10^6 were achieved (Fig. 18) at quite low overall MCP bias (~800V per MCP). Even after one year the photon pulse amplitude distribution and gain is virtually unchanged (Fig. 18). The small differences between the two measurements can be attributed to issues with the calibration of the setup. The borosilicate ALD MCPs used were from a fairly early development batch and show significant hexagonal multifiber modulation in the accumulated photon counting images (Fig. 19) and the dust/debris on them resulted in hotspots and deadspots in the images. Despite the fixed pattern noise the images are stable, and the gain is quite uniform (Fig. 19) across the detector [20]. After one year the imaging performance is essentially the same (Figs. 19, 20). Hotspot intensities have changed a little in some cases but the overall image is virtually the same. The fast pulse signals and sub nanosecond time resolution measured at the MCP output face are essentially the same as standard MCPs.

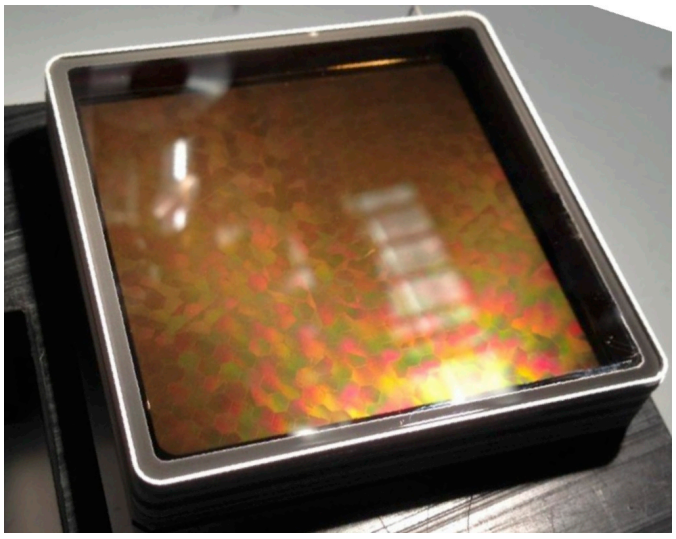

Fig. 21: Planacon 50mm detector with a bialkali cathode and a pair of 53mm, 10µm pore, 60:1 L/d, 8° bias ALD borosilicate substrate MCPs, 32 x 32 anode array.

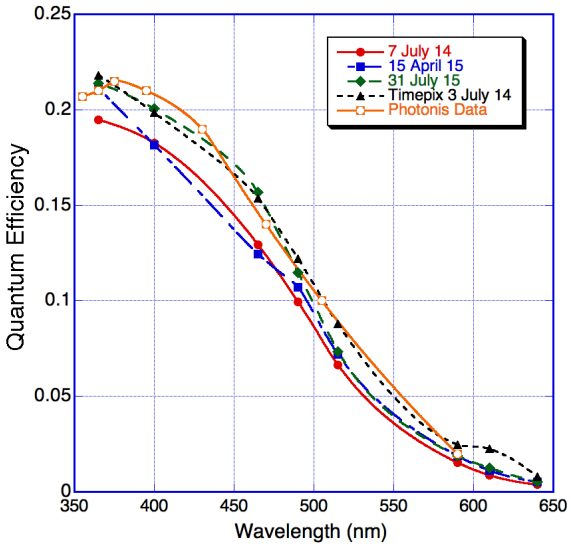

Fig. 22: Bialkali cathode quantum efficiency 12 month lifetest for a Planacon with a pair of 53mm, 10µm pore, 60:1 L/d, 8° bias ALD borosilicate substrate MCPs. Timepix planacon [21].

3.2 Planacon Tube with ALD Borosilicate Substrate Microchannel Plates

To evaluate applications of ALD MCPs we have also used them in a commercial sealed tube. The PHOTONIS Planacon is a useful format with a ~50mm active area (Fig. 21) to test basic functional parameters. The first device we have made uses a 32 x 32 anode pad array, and includes two 10 μm pore ALD MCPs with 60:1 l/d and 8° pore bias. The photocathode was a standard production bialkali, with good uniformity [20], and most of the area was within 15% of the peak quantum efficiency value. We have continued to measure the efficiency (Fig. 22) of this photocathode over a 12 month period. The initial quantum efficiency was close to the standard production expectations, and over the 12 month period our measurement have show no degradation of the photocathode and good agreement with the values supplied by PHOTONIS at the time of delivery of the tube. Further studies of imaging and timing performance are anticipated to obtain a better assessment of the performance / lifetime characteristics vs the standard MCP Planacon tubes.

4. ACKNOWLEDGEMENTS

We acknowledge the efforts of S. Jelinsky, J. Hull, J. Tedesco, T. Curtis, J. Schwarz, PHOTONIS – (Roden, Brive & Lancaster), SVT Inc. and Incom Inc. for their assistance. This work was supported by NASA grants NNG11AD54G & NNX14AD34G and DOE grant 005099.

5. REFERENCES

1. Siegmund, O.H.W., M.A. Gummin, J.M. Stock, et. al, Performance of the double delay line microchannel plate detect detectors for the Far-Ultraviolet-Spectroscopic Explorer, *Proc SPIE* 3114, pp.283-94 (1997).
2. Siegmund, O.H.W., P. Jelinsky, S. Jelinsky, et al., High resolution cross delay line detectors for the GALEX mission, *Proc. SPIE* 3765, pp.429-40 (1999).
3. Stock, J.M. O.H.W. Siegmund, J.S. Hull, et al., Cross-delay-line microchannel plate detectors for the Spectrographic Imager on the IMAGE satellite, *Proc SPIE* 3445, pp.407-14 (1998).
4. Siegmund, O.H.W., M.A. Gummin, T. Sasseen, et al., Microchannel plates for the UVCS and SUMER instruments on the SOHO satellite*, Proc. SPIE* 2518, pp.334-55 (1995).
5. Vallerga, J.; Zaninovich, J.; Welsh, B.; Siegmund, O.; McPhate, J.; Hull, J.; Gaines, G.; Buzasi, D. The FUV detector for the cosmic origins spectrograph on the Hubble Space Telescope, *Nuclear Instruments and Methods in Physics Research Section A*, Volume 477, Issue 1-3, p. 551-555 (2002).
6. Siegmund, O.H.W., J. McPhate, A. Tremsin, J.V. Vallerga, B.Y. Welsh and J.M. Wheatley, *AIP Conference Proceedings*, 984, 103 (2008).
7. Priedhorsky. W.and J. Bloch, *Applied Optics*, 44(3), 423-433 (2004).
8. Siegmund, O.H.W., J. Vallerga, P. Jelinsky, M. Redfern, X. Michalet, S. Weiss, "Cross Delay Line Detectors for High Time Resolution Astronomical Polarimetry and Biological Fluorescence Imaging", *IEEE* Nuclear Science Symposium and Medical Imaging Conference, (2005).
9. Michalet, X.; Siegmund, O. H. W.; Vallerga, J. V.; Jelinsky, P.; Millaud, J. E.; Weiss, S., Photon-counting H33D detector for biological fluorescence imaging, Nuclear Instruments and Methods, A, Vol. 567(1), p. 133 (2006).
10. Siegmund, O., J.V. Vallerga, A.S. Tremsin, J. McPhate, X. Michalet, S. Weiss, H.J. Frisch, R.G. Wagner, A. Mane, J. Elam, G. Varner. "Large Area and High Efficiency Photon Counting Imaging Detectors with High Time and Spatial Resolution for Night Time Sensing and Astronomy", Advanced Maui Optical and Space Surveillance Technologies Conference, (2012).
11. Siegmund, O.H.W. J.V. Vallerga, A. Tremsin, J. McPhate, B. Welsh "Optical Photon Counting Imaging Detectors with Nanosecond Time Resolution for Astronomy and Night Time Sensing" Advanced Maui Optical and Space Surveillance Technologies Conference Proceedings, p.E77 (2011).
12. Siegmund, O.H.W., J.B. McPhate, S.R. Jelinsky, J.V. Vallerga, A.S. Tremsin, R. Hemphill, H.J. Frisch, R.G. Wagner, J. Elam, A. Mane, "Large Area Microchannel Plate Imaging Event Counting Detectors With Sub-Nanosecond Timing," IEEE Transactions on Nuclear Science, 60(2), pp. 923-931 (2013).
13. Siegmund, O., N. Richner G. Gunjala, J.B. McPhate, A.S. Tremsin, H.J. Frisch, J. Elam, A. Mane, R. Wagner, C.A. Craven, M.J. Minot, *Proc. SPIE* 8859, 88590Y (2013).
14. Siegmund, O., J. McPhate, A.S. Tremsin, J.V. Vallerga, H.J. Frisch, R.G. Wagner, A. Mane, J. Elam, G. Varner. "Large Area flat panel Photon Counting Imaging Detectors for Astronomy and Night Time Sensing", Advanced Maui Optical and Space Surveillance Technologies Conference, (2013).
15. Mane. A. Q. Peng, J.W. Elam, D.C. Bennis, C.A. Craven, M.A. Detarando, J.R. Escolas, H.J. Frisch, S.J. Jokela, J. McPhate, M.J. Minot, O.H.W. Siegmund, J.M. Renaud, R.G. Wagner, and M. J. Wetstein "A novel atomic layer

deposition method to fabricate economical and robust large area microchannel plates for photodetectors," Physics Procedia 37, 722 – 732 (2012).
16. Fraser, G.W. "X-ray detectors in astronomy", Cambridge University Press, 1989.
17. C. Ertley, O. H. W. Siegmund, J. Schwarz, A. U. Mane, M. J. Minot[c] A. O'Mahony, C. A. Craven, M. Popecki *Proc SPIE* 9601, (2015)
18. Siegmund, O., Vallerga, J., Welsh, B., McPhate, J., Rogers, D. "High Speed Optical Imaging Photon Counting Microchannel Plate Detectors for Astronomical and Space Sensing Applications", Advanced Maui Optical and Space Surveillance Technologies Conference Proceedings. p.90 (2009).
19. Siegmund, O., Vallerga, J., Welsh, B., Tremsin, A., McPhate, J., "High Spatial resolution GaN and Optical Photon Counting Detectors with sub-nanosecond timing for Astronomical and Space Sensing Applications", Advanced Maui Optical and Space Surveillance Technologies Conference. p.69 (2008).
20. Siegmund, O.H.W., J.V. Vallerga, A.S. Tremsin, J. Hull, J. Elam, A. Mane, A O'Mahony, **"**Optical and UV Sensing Sealed Tube Microchannel Plate Imaging Detectors with High Time Resolution", Advanced Maui Optical and Space Surveillance Technologies Conference, (2014).
21. Vallerga, J.; Tremsin, A.; DeFazio, J.; Michel, T.; Alozy, J.; Tick, T.; Campbell, M. "Optical MCP image tube with a quad Timepix readout: initial performance characterization", Journal of Instrumentation, 9(5), C05055 (2014).